Eur. J. Mech., A/Solids, **14**, n° 5, 747-771, 1995

Strain localization in single crystals: bifurcation analysis, effects of boundaries and interfaces

S. FOREST and G. CAILLETAUD*

ABSTRACT. – The bifurcation theory in elastoplasticity at large strain has been extensively used in the past to model the development of shear bands in ductile single crystals. In contrast we perform here a bifurcation analysis for single crystals undergoing symmetric multiple slip at small strain with a view to modelling slip band formation during incipient plasticity. In that case strain softening is required for such bifurcation modes to occur. The actual three-dimensional geometry of f.c.c. single crystals is taken into account and slip configurations are considered for which 1, 2, 4, 6 or 8 slip systems are simultaneously activated. Three-dimensional finite element calculations are carried out to induce the occurrence of some of the predicted bifurcation modes in a one-element thick single crystal plate in tension. Viscoplasticity is used to reduce the mesh dependence of the results. To trigger localization geometrical imperfections are introduced as usually done in the literature but we also introduce material flaws, such as slightly lower local yield stress, because it is thought to be physically more relevant.

A bifurcation analysis at boundaries and interfaces is then performed in the case of single slip. It is proved firstly that no deviation occurs when a slip band regarded as a single slip bifurcation mode reaches a boundary and secondly that equilibrium conditions allow the crossing of an interface between two crystals as soon as localization conditions are fulfilled on each side. Finite element simulations of the crossing of a grain boundary separating two misoriented single crystals are presented. Finally the results of some finite element calculations indicate that a slip band initiated in a domain of a single crystal with a softening behaviour can propagate through neighbouring hardening zones. This provides a better understanding of the mechanisms associated with slip band initiation and propagation.

1. Introduction

Plastic deformation of single crystals induced by dislocation motion is intrinsically a heterogeneous process. However the glide of dislocations on discrete slip planes often results in homogeneous macroscopic deformation, so that crystal plasticity can be successfully described within the framework of continuum mechanics. Initially homogeneous deformation may nevertheless give way to localized deformation patterns. Shear bands for instance that may appear in ductile single crystals after sufficient straining and that eventually lead to fracture, have been extensively studied in the literature and are usually regarded as bifurcation modes in the constitutive description of the mechanical behaviour of single crystals at large strain [Asaro & Rice, 1977]. Numerical simulations of shear banding have been provided in [Peirce *et al.*, 1982 and 1983] in the case of planar double slip. This simplified slip geometry corresponds only approximately to actual double slip in f.c.c. and b.c.c. single crystals.

Localized deformation can also arise at the very beginning of plastic flow with the formation of intense slip bands, sometimes called coarse slip bands. In that case the

* Centre des Matériaux, URA CNRS 866, École des Mines de Paris, 91003 Evry, France.

EUROPEAN JOURNAL OF MECHANICS, A/SOLIDS, VOL. 14, N° 5, 1995
0997-7538/95/05/$ 4.00/© Gauthier-Villars

prediction of the bifurcation modes does not require an analysis at large strain. In the following we perform a bifurcation analysis for symmetric multiple slip configurations in single crystals at small strain. The bifurcation modes and critical hardening moduli are determined for the actual three-dimensional f.c.c. geometry when 1, 2, 4, 6 or 8 slip systems are simultaneously activated. Then three-dimensional finite element calculations are carried out to simulate some of the predicted bifurcation modes. To trigger localization we introduce geometrical imperfections, as usually done in the literature, or material flaws, such as a slightly non homogeneous yield stress.

Finally we tackle the problem of single slip bifurcation modes at a boundary and interface. In particular we investigate numerically whether non homogeneous deformation at a grain boundary due to strain incompatibility in a bicrystal may or not hamper slip band propagation.

2. Bifurcation analysis for single crystals undergoing symmetric multiple slip

2.1. Incremental formulation of the constitutive equations in elastoplasticity

In single crystals, the plastic strain rate is the sum of the contributions of each slip system according to:

$$\underset{\sim}{\dot{\varepsilon}}^p = \sum_{g=1}^{12} \dot{\gamma}^g \{\underline{s}^g \otimes \underline{z}^g\} \tag{2.1}$$

where $\underline{s}$ and $\underline{z}$ respectively are the slip direction, the normal to the slip plane. The braces { } denote symmetrization and $\otimes$ the tensor product. We consider here the 12 octahedral slip systems of f.c.c. crystals. Schmid's law written for each slip system gives a yield surface with vertexes:

$$\tau^g - \tau_c^g \leq 0 \qquad \text{with} \quad \tau^g = \underset{\sim}{\sigma} : (\underline{s}^g \otimes \underline{z}^g). \tag{2.2}$$

Mandel's hardening rule involves an interaction matrix to describe self- or latent hardening:

$$\dot{\tau}_c^s = \sum_{g=1}^{12} h^{sg} |\dot{\gamma}^g|. \tag{2.3}$$

In the particular case of single crystals in tension undergoing symmetric multiple slip, the previous expressions simplify, providing that we take a simple form for the interaction matrix:

$$\underset{\sim}{\dot{\varepsilon}}^p = \dot{\gamma} \underset{\sim}{\mathbf{P}} \qquad \text{with} \quad \dot{\gamma} > 0 \tag{2.4}$$

$$\dot{\tau}^s = \dot{\tau}_c = H\dot{\gamma} \qquad \forall s \in A \tag{2.5}$$

where

$$\underset{\sim}{\mathbf{P}} = \sum_{g \in A} \{\underline{s}^g \otimes \underline{z}^g\} \tag{2.6}$$

and

$$H = mh \qquad \text{if} \quad h^{ij} = h \qquad \forall i, j \text{ (isotropic hardening)};$$
$$H = h \qquad \text{if} \quad h^{ij} = h\,\delta^{ij} \text{ (self-hardening)}.$$

In the previous expressions $A \subset \{1, \ldots, 12\}$ contains the indices of the m active slip systems. The elastic part of the deformation obeys Hooke's law:

$$\dot{\underset{\sim}{\sigma}} = \underset{\approx}{\mathbf{E}} : \dot{\underset{\sim}{\varepsilon}}^e \tag{2.7}$$

where $\underset{\approx}{\mathbf{E}}$ is the definite positive four-rank elasticity tensor and has the usual symmetry properties. Combining equations (2.1) to (2.6) yields:

$$\dot{\gamma} = \frac{\underset{\sim}{\mathbf{P}} : \underset{\approx}{\mathbf{E}} : \dot{\underset{\sim}{\varepsilon}}}{H + \underset{\sim}{\mathbf{P}} : \underset{\approx}{\mathbf{E}} : \underset{\sim}{\mathbf{P}}}. \tag{2.8}$$

Thereby plastic loading occurs for $\underset{\sim}{\mathbf{P}} : \underset{\approx}{\mathbf{E}} : \dot{\underset{\sim}{\varepsilon}} > 0$ and we assume that $H + \underset{\sim}{\mathbf{P}} : \underset{\approx}{\mathbf{E}} : \underset{\sim}{\mathbf{P}} > 0$ (no snap-back behaviour). It is then possible to derive a linear rate formulation of the elastoplastic constitutive equations:

$$\dot{\underset{\sim}{\sigma}} = \underset{\approx}{\mathbf{L}} : \dot{\underset{\sim}{\varepsilon}} \tag{2.9}$$

where

$$\underset{\approx}{\mathbf{L}} = \underset{\approx}{\mathbf{E}} - \frac{(\underset{\approx}{\mathbf{E}} : \underset{\sim}{\mathbf{P}}) \otimes (\underset{\sim}{\mathbf{P}} : \underset{\approx}{\mathbf{E}})}{H + \underset{\sim}{\mathbf{P}} : \underset{\approx}{\mathbf{E}} : \underset{\sim}{\mathbf{P}}} \tag{2.10}$$

under plastic loading.

2.2. Bifurcation modes involving strain rate jumps

We investigate the possibility of the emergence of deformation modes involving jumps of the strain rate across a given surface S with normal $\underline{n}$. To be compatible the jump of the strain rate must be of the form:

$$\exists\, \underline{g} \quad \text{such that} \quad [\![\dot{\underset{\sim}{\varepsilon}}]\!] = \{\underline{g} \otimes \underline{n}\} \tag{2.11}$$

according to Hadamard's compatibility condition [Hadamard, 1903]. The brackets [![ ]!] denote the difference of the limit values on each side of S.

Continuing equilibrium across S requires:

$$[\![\dot{\underset{\sim}{\sigma}}]\!]\,\underline{n} = \underline{0}. \tag{2.12}$$

If plastic loading occurs on each side of S, the bifurcation modes are called continuous localization modes and necessary conditions for such modes to become possible inside the body have been worked out by Rice [1976]:

$$\det \underline{n} \cdot \underset{\approx}{\mathbf{L}} \cdot \underline{n} = 0. \tag{2.13}$$

Bifurcation becomes possible for a critical hardening modulus given by:

$$H\,(\underline{n}) = -\underset{\sim}{\mathbf{P}} : \underset{\approx}{\mathbf{E}} : \underset{\sim}{\mathbf{P}} + (\underset{\sim}{\mathbf{P}} : \underset{\approx}{\mathbf{E}} \cdot \underline{n})\,(\underline{n} : \underset{\approx}{\mathbf{E}} \cdot \underline{n})^{-1}\,(\underline{n} \cdot \underset{\approx}{\mathbf{E}} : \underset{\sim}{\mathbf{P}}) \tag{2.14}$$

and the direction of $\underline{g}$ is then:

$$\underline{g} \propto (\underline{n} \cdot \underset{\approx}{\mathbf{E}} \cdot \underline{n})^{-1}\,(\underline{n} \cdot \underset{\approx}{\mathbf{E}} : \underset{\sim}{\mathbf{P}}) \tag{2.15}$$

its magnitude being left arbitrary in this model. If elastic unloading occurs on one side of S, the associated bifurcation modes are called discontinuous localization modes. Borré & Maier [1989] extended the results established by Rice & Rudnicki [1980] and proved that in the case of usual elastoplastic materials for which the work-hardening rate decreases with strain, a discontinuous localization mode involving elastic unloading cannot occur before the condition for continuous bifurcation modes (2.13) is fulfilled. A proof of this result can also be found in [Ottosen & Runesson, 1991].

Accordingly the critical hardening modulus for which a localized deformation mode may occur for the first time is obtained by solving:

$$H^{cr} = \sup_{\|\underline{n}\|=1} H\,(\underline{n}). \tag{2.16}$$

The orientation of the first possible band of localized deformation is then given by the values of $\underline{n}$ for which H^{cr} is reached. The problem reduces to maximizing the Lagrangian function:

$$L\,(\underline{n},\,\lambda) = H\,(\underline{n}) - \lambda\,(\|\underline{n}\|^2 - 1). \tag{2.17}$$

We refer to the method developed in [Bigoni & Hueckel, 1991] to solve this maximization problem for general non associated elastoplasticity. But the present analysis is restricted

to associated and incompressible plasticity. Equation (2.17) combined with (2.14) and written in the principal axes of $\underset{\sim}{\mathbf{P}}$ then becomes:

$$L\,(\underline{n},\,\lambda) = 2\mu\left(2\,n_i^2 P_i^2 - \sum_{i=1}^{3} P_i^2 - \frac{1}{1-\nu}\,(n_i^2 P_i)^2\right) - \lambda\left(\sum_{i=1}^{3} n_i^2 - 1\right) \tag{2.18}$$

for isotropic elasticity, μ and ν being respectively the shear modulus and Poisson's ratio. Writing $\dfrac{\partial L}{\partial \lambda} = \dfrac{\partial L}{\partial n_k} = 0$ makes the problem equivalent to the resolution of the system:

$$n_k\left(P_k^2 - \frac{1}{1-\nu}\,(n_i^2 P_i)\,P_k - \frac{\lambda}{4\mu}\right) = 0 \qquad k \in \{1,\,2,\,3\}. \tag{2.19}$$

If $n_1\,n_2\,n_3 \neq 0$, the system is indeterminate or impossible depending on P_1, P_2, P_3.
If $n_k = 0$ and $n_i\,n_j \neq 0$,
if $P_i = P_j$, the system is indeterminate;
if $P_i \neq P_j$,

$$n_i^2 = \frac{P_i + \nu P_k}{P_i - P_j} \qquad \text{and} \qquad n_j^2 = 1 - n_i^2. \tag{2.20}$$

The jump of the strain rate across the surface with normal $\underline{n}$ is also described by $\underline{g}$:

$$\begin{cases} g_i = (P_i - P_j)\,n_i \\ g_j = (P_j - P_i)\,n_j \\ g_k = 0 \end{cases} \tag{2.21}$$

$$\begin{cases} [\![\dot{\underset{\sim}{\varepsilon}}_i]\!] = P_i + \nu P_k \\ [\![\dot{\underset{\sim}{\varepsilon}}_j]\!] = P_j + \nu P_k \\ [\![\dot{\underset{\sim}{\varepsilon}}_k]\!] = 0 \end{cases} \tag{2.22}$$

the corresponding critical hardening modulus being

$$H^{cr} = -E P_k^2 \tag{2.23}$$

where E is Young's modulus.
If $n_i^2 = 1$ and $n_j = n_k = 0$,

$$H^{cr} = -2\mu\left(\frac{(P_j + \nu P_k)^2}{1-\nu} + (1+\nu)\,P_k^2\right). \tag{2.24}$$

The first possible band is given by the combination i, j, k for which H^{cr} has the highest value.

2.3. Application to F.C.C. single crystals

Single Slip

For a f.c.c.single crystal in tension in the direction [123] for instance, the slip system $B4$ is active according to the Schmid & Boas notation, so that, in the crystallographic axes:

$$P = \frac{1}{\sqrt{6}} \begin{bmatrix} -1 & -1/2 & 0 \\ -1/2 & 0 & 1/2 \\ 0 & 1/2 & 1 \end{bmatrix}. \tag{2.25}$$

The eigenvectors are

$$a_1 = \begin{bmatrix} \frac{1}{\sqrt{6}} \\ \frac{-2}{\sqrt{6}} \\ \frac{1}{\sqrt{6}} \end{bmatrix}; \quad a_2 = \frac{1}{2\sqrt{15-6\sqrt{6}}} \begin{bmatrix} -5+2\sqrt{6} \\ \sqrt{6}-2 \\ 1 \end{bmatrix}; \tag{2.26}$$

$$a_3 = \frac{1}{2\sqrt{15+6\sqrt{6}}} \begin{bmatrix} -5-2\sqrt{6} \\ -\sqrt{6}-2 \\ 1 \end{bmatrix}.$$

The eigenvalues are respectively 0, 1/2, –1/2. In the reference system $(\underline{a}_1, \underline{a}_2, \underline{a}_3)$, the components of $\underline{g}$ and $\underline{n}$ characterizing the bifurcation modes are, according to (2.20) and (2.21):

$$\begin{cases} n_1 = 0 \\ n_2 = \frac{1}{\sqrt{2}} \\ n_3 = \pm\frac{1}{\sqrt{2}} \end{cases}; \quad \begin{cases} g_1 = 0 \\ g_2 = n_2 \\ g_3 = -n_3 \end{cases}$$

In the crystallographic reference system, this gives

$$n = \frac{1}{\sqrt{3}} \begin{bmatrix} 1 \\ 1 \\ 1 \end{bmatrix} \quad \text{or} \quad n = \frac{1}{\sqrt{2}} \begin{bmatrix} -1 \\ 0 \\ 1 \end{bmatrix}. \tag{2.27}$$

Thus deformation can localize on the slip plane and on the plane normal to the slip direction which is referred to as a *kink plane* in literature. The bifurcation modes are possible as soon as

$$H = H^{cr} = 0. \tag{2.28}$$

An analysis at finite strain does not essentially affect these results [Asaro & Rice, 1977].

Double Slip

It the tensile direction is [012], slip systems $B4$ and $A3$ are simultaneously activated so that:

$$P = \frac{1}{\sqrt{6}} \begin{bmatrix} -2 & 0 & 0 \\ 0 & 0 & 1 \\ 0 & 1 & 2 \end{bmatrix}. \tag{2.29}$$

The eigenvectors are

$$a_1 = \begin{bmatrix} 1 \\ 0 \\ 0 \end{bmatrix}; \quad a_2 = \frac{1}{\sqrt{2}\sqrt{2-\sqrt{2}}} \begin{bmatrix} 0 \\ 1 \\ 1-\sqrt{2} \end{bmatrix}; \tag{2.30}$$

$$a_3 = \frac{1}{\sqrt{2}\sqrt{2+\sqrt{2}}} \begin{bmatrix} 0 \\ 1 \\ 1+\sqrt{2} \end{bmatrix}.$$

The eigenvalues are respectively $-\sqrt{2/3}$, $\sqrt{1/6}-\sqrt{1/3}$, $\sqrt{1/6}+\sqrt{1/3}$. In the reference system $(\underline{a}_1, \underline{a}_2, \underline{a}_3)$, the components of $\underline{n}$ characterizing the bifurcation modes are:

$$\begin{cases} n_1^2 = \frac{1+\sqrt{2}+\nu(1-\sqrt{2})}{3+\sqrt{2}} \\ n_2^2 = 0 \\ n_3^2 = 1-n_1^2 \end{cases} \tag{2.31}$$

$$H^{cr} = -E\,(\sqrt{1/6}-\sqrt{1/3})^2 \tag{2.32}$$

A very low value of the hardening modulus must be reached for compatible bifurcation modes to become possible. Furthermore the bifurcation planes are non crystallographic and depend on Poisson's ratio.

The situation of symmetric double slip has been extensively studied for large strains by Asaro [1979] and Peirce *et al.* [1982], though in the case of a planar model of single crystals that does not correspond to any real physical situation. These authors also found non crystallographic bifurcation planes. Peirce [1983] considered the actual 3D geometry of a single crystal undergoing symmetric double slip. He found bifurcation modes for which one system is under plastic loading whereas the other is under neutral loading. Instead, in the previous analysis, we investigated modes for which the two systems are equally active. The solution proposed by Peirce gives bifurcation planes close to the slip or kink planes.

Four Slip Systems

If the tensile direction is [011], slip systems $B4$, $A3$ $B5$ and $A6$ are simultaneously activated so that:

$$P = \frac{4}{\sqrt{6}} \begin{bmatrix} -1 & 0 & 0 \\ 0 & 1/2 & 1/2 \\ 0 & 1/2 & 1/2 \end{bmatrix}. \tag{2.33}$$

$$a_1 = \begin{bmatrix} 1 \\ 0 \\ 0 \end{bmatrix}; \quad a_2 = \frac{1}{\sqrt{2}} \begin{bmatrix} 0 \\ 1 \\ -1 \end{bmatrix}; \quad a_3 = \frac{1}{\sqrt{2}} \begin{bmatrix} 0 \\ 1 \\ 1 \end{bmatrix}. \tag{2.34}$$

The eigenvalues are respectively $-\frac{4}{\sqrt{6}}$, 0, $\frac{4}{\sqrt{6}}$. In the reference system $(\underline{a}_1, \underline{a}_2, \underline{a}_3)$, the components of $\underline{n}$ characterizing the bifurcation modes are:

$$\begin{cases} n_1^2 = 1/2 \\ n_2^2 = 0 \\ n_3^2 = 1/2 \end{cases}$$

In the crystallographic reference system, this gives

$$n = \begin{bmatrix} \frac{1}{\sqrt{2}} \\ 1/2 \\ 1/2 \end{bmatrix} \quad \text{or} \quad n = \begin{bmatrix} \frac{-1}{\sqrt{2}} \\ 1/2 \\ 1/2 \end{bmatrix}. \tag{2.35}$$

$$H^{cr} = 0. \tag{2.36}$$

Once more, bifurcation planes are non crystallographic but independent of ν. The critical hardening modulus is zero. This slip configuration is therefore prone to localization.

Six Slip Systems

If the tensile direction is [111], the slip systems $A3$, $A6$, $C1$, $C3$, $D1$, and $D6$ are theoretically simultaneously activated so that:

$$P = \frac{2}{\sqrt{6}} \begin{bmatrix} 0 & 1 & 1 \\ 1 & 0 & 1 \\ 1 & 1 & 0 \end{bmatrix} \tag{2.37}$$

$$a_1 = \frac{1}{\sqrt{3}} \begin{bmatrix} 1 \\ 1 \\ 1 \end{bmatrix}; \quad a_2 = \frac{1}{\sqrt{2}} \begin{bmatrix} 0 \\ 1 \\ -1 \end{bmatrix}; \quad a_3 = \frac{1}{\sqrt{6}} \begin{bmatrix} -2 \\ 1 \\ 1 \end{bmatrix}. \tag{2.38}$$

The eigenvalues are respectively $\frac{4}{\sqrt{6}}$, $\frac{-2}{\sqrt{6}}$, $\frac{-2}{\sqrt{6}}$. In the reference system $(\underline{a}_1, \underline{a}_2, \underline{a}_3)$, the components of $\underline{n}$ characterizing the bifurcation modes are:

$$\begin{cases} n_1^2 = \frac{2-\nu}{3} \\ n_2^2 = \frac{1+\nu}{3} \\ n_3^2 = 0 \end{cases} \tag{2.39}$$

$$H^{cr} = -\frac{2}{3} E. \tag{2.40}$$

The critical hardening modulus is very low and the bifurcation planes are non crystallographic.

Eight Slip Systems

If the tensile direction is [001], the slip systems $A2$, $A3$, $B2$, $B4$, $C1$, $C3$, $D1$, and $D4$ are theoretically simultaneously activated so that:

$$P = \frac{8}{\sqrt{6}} \begin{bmatrix} -1/2 & 0 & 0 \\ 0 & -1/2 & 0 \\ 0 & 0 & 1 \end{bmatrix} \tag{2.41}$$

$$\begin{cases} n_1^2 = \frac{1+\nu}{3} \\ n_2^2 = 0 \\ n_3^2 = \frac{2-\nu}{3} \end{cases} \tag{2.42}$$

$$H^{cr} = -\frac{4}{3} E. \tag{2.43}$$

The previous analysis shows that crystallographic bifurcation planes are obtained only in the case of single slip and that slip configuration for which 1 or 4 slip systems are activated, are the most prone to localization. It is clear that if $H^{cr} \ll 0$, diffuse bifurcation modes, or modes for which slip does not remain identical on all active systems, are likely to develop.

3. Finite element simulations of localized deformation using a viscoplastic model for single crystals

3.1. Viscoplasticity and mesh dependence

Bifurcation condition (2.13) corresponds to the loss of ellipticity of the partial differential equations of equilibrium ([Hill & Hutchinson, 1975]). That is why simulations

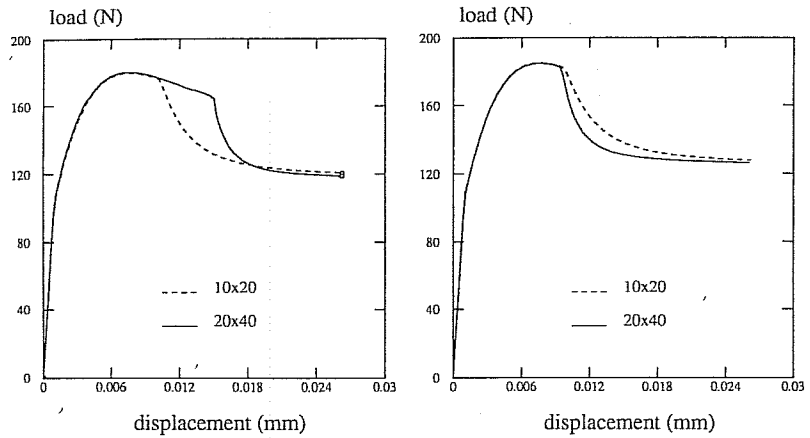

Fig. 1. – Load-displacement curves of a flawed plate in tension: mesh dependence. Results obtained with two different meshes involving respectively 200 and 800 rectangular elements with quadratic interpolation are compared in the case of (*a*) elastoplasticity (left) and (*b*) elastoviscoplasticity (right).

of localization of deformation using finite element calculations exhibit a strong mesh dependence. Various regularization methods have been developped to restore the well-posedness of the problem, including the use of non-local, higher order gradient or Cosserat continua (*see* [De Borst, 1991]), [De Borst *et al.*, 1993]). In the dynamic case Harirêche and Loret [1992] introduce viscoplasticity as a regularization procedure. We show here that viscoplasticity can be introduced in the static case to significantly reduce the mesh dependence of the results. We have first considered the tensile loading of a plate under plane stress conditions. To trigger localization at small strain within the framework of associated plasticity, a softening behaviour is required and a slight geometrical flaw is introduced on the side of the plate. The presence of the geometrical imperfection induces shear band formation after the peak of the load-displacement curve, associated with a sharp load drop. In elastoplasticity, the thickness of the band and the bifurcation point are mesh dependent. Figure 1 shows that viscosity significantly reduces these spurious effects. Very high viscosity may even preclude localization. For these preliminary calculations we have used classical viscoplastic phenomenological models of the form:

$$\dot{v} = \left\langle \frac{J_2\left(\underset{\sim}{\sigma} - \underset{\sim}{\mathbf{X}}\right) - R}{K} \right\rangle^n \tag{3.1}$$

where v is the equivalent viscoplastic strain, J_2 the second invariant and $\underset{\sim}{\mathbf{X}}$ and R are hardening variables (*see* [Lemaitre & Chaboche, 1985]). The regularization role of viscoplasticity regarding the thickness of localization bands is illustrated in Figure 2. In the following viscoplasticity is introduced in the modelling of the behaviour of single crystals.

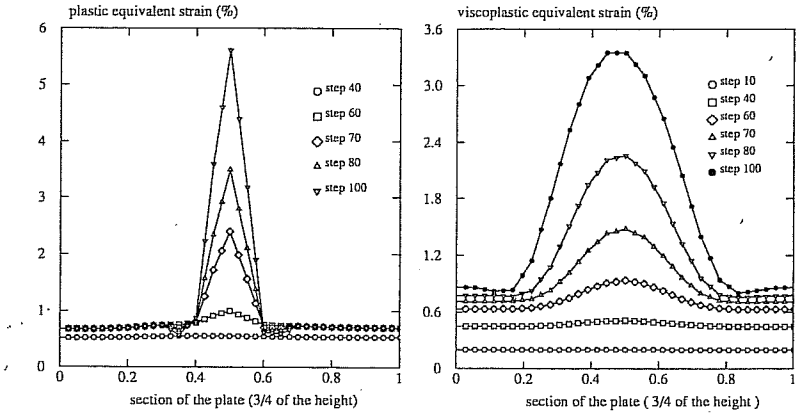

Fig. 2. – Formation of a localized deformation band in a flawed plate in tension with prescribed displacement at constant rate. The profile of deformation along a section of the plate is shown for several steps of the calculation in the case of (*a*) elastoplasticity and (*b*) elastoviscoplasticity.

3.2. Equations of the model

This model has been developped and implemented in a finite element code by Méric & Cailletaud [1991] to describe the complex behaviour of nickel-base single crystal superalloys under monotonic and cyclic loading at various temperatures. The shear strain rate on each slip system is given by:

$$\dot{\gamma}^s = \left\langle \frac{|\tau^s - x^s| - r^s}{k} \right\rangle^n \operatorname{sign}\left(\tau^s - x^s\right) \tag{3.2}$$

where k and n are viscosity parameters. Isotropic and kinematic hardening variables are attributed to each slip system and obey the following evolution rules:

Local isotropic hardening

$$r^s = r_0 + Q \sum_{r=1}^{N} h^{sr}\left(1 - \exp\left(-b v^r\right)\right) \qquad \text{with} \quad \dot{v}^s = |\dot{\gamma}^s|; \tag{3.3}$$

Local kinematic hardening

$$x^s = c\,\alpha^s \qquad \text{with} \quad \dot{\alpha}^s = \dot{\gamma}^s - d\,\dot{v}^s \alpha^s. \tag{3.4}$$

3.3. Results

We consider the tension of a one-element thick rectangular f.c.c. single crystal plate. The elements are 20–node bricks with 27 Gauss points. The tensile direction coincides successively with various crystallographic directions so as to induce single or multiple slip. To trigger localization we introduce a geometrical imperfection on one side of the plate:

$$x_1 = l\left(1 + a\left(\tanh\frac{\omega\,(x_3 - x_0)^2}{L^2} - 1\right)\right) \tag{3.5}$$

with 1 and 3 denoting respectively the width and length directions of the plate. We take $a = 0.002$, $\omega = 25$ and allow $\frac{L}{l}$ to vary between 1.5 and 3. x_0 determines the position of the geometrical flaw along the length of the specimen.

The material parameters have been chosen so that the competition between the two non linear hardening variables leads to an initial hardening followed by a softening behaviour:

$$E = 200\,000\ \text{MPa} \quad r_0 = 50\ \text{MPa} \quad c = 20\,000\ \text{MPa} \quad k = 5\ \text{MPa}\ s^{1/n}$$
$$\nu = 0.3 \quad Q = -45\ \text{MPa} \quad d = 900 \quad n = 2$$
$$b = 210.$$

With this set of parameters softening occurs after small straining. For all orientations of the single crystals, an initial rather homogeneous deformation pattern gives way after the peak of the load-displacement curve to localization in narrow bands. The calculations have been performed with very low viscosity so that localization of deformation is accompanied by a sharp load drop. The orientations of the bands found for several single and multislip configurations are compared with the predicted ones in Table 1.

TABLE I. – Comparison between slip plane traces in the plane of the plate ($\underline{x}_1$, $\underline{x}_3$), predicted bifurcation band traces and localization band traces obtained by the FE analysis, for various multislip configurations. A, B, C and D denote respectively slip planes $[\bar{1}11]$, $[111]$, $[\bar{1}\,\bar{1}1]$ and $[1\bar{1}1]$ according to the Schmid & Boas notation. Orientations are given with respect to $\underline{x}_3$ and angles are positive from $\underline{x}_3$ to $\underline{x}_1$.

Number of active slip systems;	crystal orientation $\underline{x}_3$, $\underline{x}_1$	slip planes orientation	predicted bifurcation orientation	observed bifurcation orientation	figures
1	[1 2 3]	A 50°	50°	50°	3,4 *a*
	[6 3 $\bar{4}$]		–77°	–76°	
2	[0 1 2]	A 61°	–47°	–49°	4 *b*
	[5 2 $\bar{1}$]	B –50°	45°	47°	5 *a*
4	[0 1 1]	A 55°	45°	45°	5 *b*
	[1 0 0]	B –55°	–45°	–45°	
8	[0 0 1]	A, C 45°	55°	53°	5 *c*
	[1 0 0]	B, D –45°	–55°	–53°	

Single Slip

The length of the plate coincides with the [1 2 3] crystallographic direction and the perpendicular direction in the plane of the plate with [6 3 $\bar{4}$]. On Figure 3 *a* two bands of intense deformation have formed, intersecting at the location of the initial geometrical flaw. One lies on the slip plane, the other one on the kink plane, as predicted by the bifurcation analysis for single slip. The postbifurcation behaviour is characterized by the predominance of one of the two bands (*Fig.* 3 *b*). In the deformed state shown on Figure 3 *c*, displacements have been significantly magnified. Since the single crystal is misoriented, the strain field is really three-dimensional, which can be seen on Figure 4 *a*.

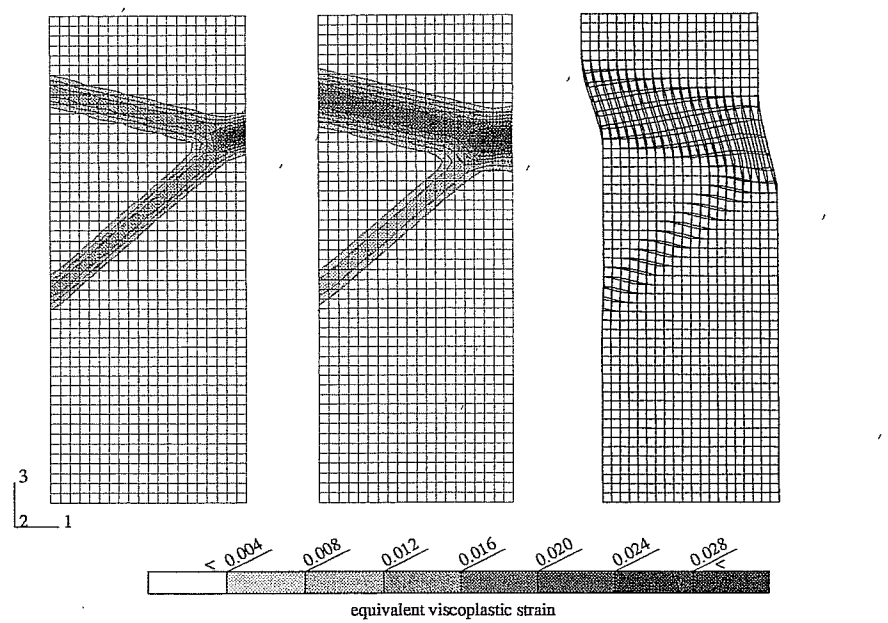

Fig. 3. – Slip and kink band formation in a single crystal plate in tension oriented for single slip. (*a*) and (*b*) contour of viscoplastic strain for two successive steps of the calculation, (*c*) final deformed state (magnified by 20).

Double Slip

In this case (*Figs.* 4 *a* and 5 *a*), the planes of localized deformation are not crystallographic, as expected. The orientations given by formula (2.31) change only by 2 or 3° when ν varies between 0 and 0.5, so that the dependence on ν could not be precisely detected. Figure 4 *b* shows that in the case of symmetric double slip, the strain field is strongly three-dimensional.

Four Slip Systems

In the configuration of Figure 5 *b*, the plane (0 1 1) satisfies the plane strain condition. That is why bands of localized deformation are expected to develop at 45°.

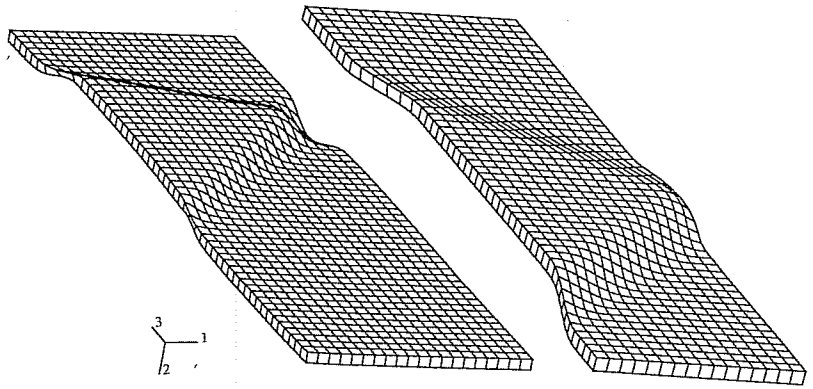

Fig. 4. – Three-dimensional displacement field of two flawed single crystal plates in tension, after strain localization. These deformated states are presented with a magnification of 15. The plates are respectively oriented for (*a*) single slip and (*b*) symmetric double slip.

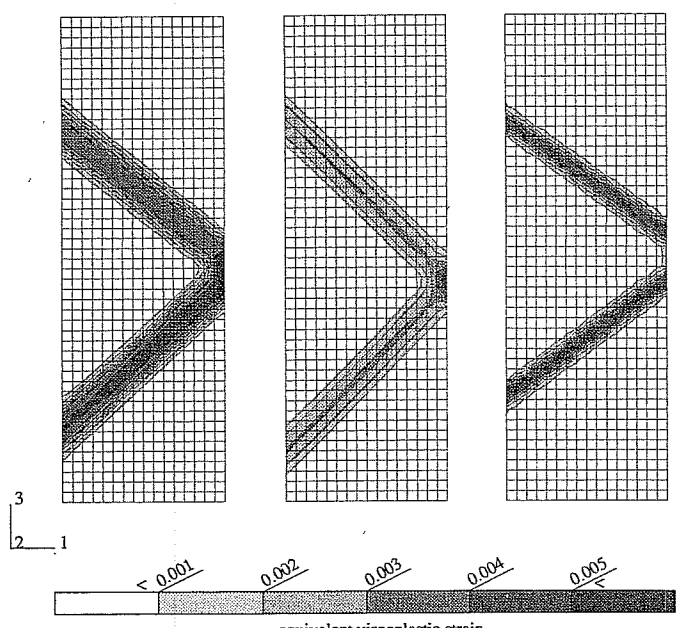

Fig. 5. – Localization band formation in single crystal plates in tension with (*a*) two, (*b*) four, (*c*) eight active slip systems.

Eight Slip Systems

This multislip configuration gives the same macroscopic deformation field as that for isotropic polycrystals in tension. The compatible bifurcation modes expected correspond to localization bands oriented at an angle θ from the tensile direction [0 0 1]:

$$\tan^2 \theta = \frac{2-\nu}{1+\nu} \tag{3.6}$$

after formula (2.42). θ ranges from 54.7° to 45° when ν varies between 0 and 0.5. For $\nu = 0.3$, $\theta \simeq 49°$. This deformation mode is only compatible for a very low negative hardening modulus.

Instead, Figure 5*c* shows that two bands formed at about 53° from the tensile axis and this happens slightly after the peak of the load-displacement curve. In fact this deformation mode is close to the shear bands at 54.7°, that are classical in the plasticity of isotropic materials. This is a diffuse bifurcation mode, which can appear as soon as the hardening modulus vanishes (*see* [Forest & Cailletaud, 1993]).

4. Effect of boundaries on localization in single crystals

4.1. Bifurcation condition at a boundary

Benallal *et al.* [1990] have searched for necessary and sufficient conditions for a strain rate discontinuity surface S to appear at, or to reach, the boundary of a solid. Besides conditions (2.11) and (2.12) inside the body, the following conditions at the boundary with normal $\underline{m}$ and where only surface forces $\underline{F}$ are applied, must be added:

$$\dot{\underset{\sim}{\sigma}}_2 \underline{m} = \dot{\underset{\sim}{\sigma}}_1 \underline{m} = \dot{\underline{F}} \tag{4.1}$$

and therefore

$$[\![\dot{\underset{\sim}{\sigma}}]\!] \underline{m} = 0. \tag{4.2}$$

For a continuous bifurcation mode, this implies:

$$(\underline{m} \cdot \underset{\approx}{\mathbf{L}} \cdot \underline{n})\, \underline{g} = 0. \tag{4.3}$$

Combining (2.10), (2.14) and (2.15) with this last condition, we obtain:

$$(\underline{m} \cdot \underset{\approx}{\mathbf{L}} \cdot \underline{n})\, \underline{g} = (\underline{m} \cdot \underset{\approx}{\mathbf{E}} \cdot \underline{n})\, (\underline{n} \cdot \underset{\approx}{\mathbf{E}} \cdot \underline{n})^{-1}\, (\underline{n} \cdot \underset{\approx}{\mathbf{E}} \cdot \underset{\sim}{\mathbf{P}}) - \frac{\underline{m} \cdot (\underset{\approx}{\mathbf{E}} : \underset{\sim}{\mathbf{P}}) \otimes (\underset{\sim}{\mathbf{P}} : \underset{\approx}{\mathbf{E}}) \cdot \underline{n}}{(\underset{\sim}{\mathbf{P}} : \underset{\approx}{\mathbf{E}} \cdot \underline{n})\, (\underline{n} \cdot \underset{\approx}{\mathbf{E}} \cdot \underline{n})^{-1}\, (\underline{n} \cdot \underset{\approx}{\mathbf{E}} : \underset{\sim}{\mathbf{P}})}\, (\underline{n} \cdot \underset{\approx}{\mathbf{E}} \cdot \underline{n})^{-1}\, (\underline{n} \cdot \underset{\approx}{\mathbf{E}} : \underset{\sim}{\mathbf{P}})$$

$$(\underline{m} \cdot \underset{\approx}{\mathbf{L}} \cdot \underline{n})\, \underline{g} = (\underline{m} \cdot \underset{\approx}{\mathbf{E}} \cdot \underline{n})\, (\underline{n} \cdot \underset{\approx}{\mathbf{E}} \cdot \underline{n})^{-1}\, (\underline{n} \cdot \underset{\approx}{\mathbf{E}} : \underset{\sim}{\mathbf{P}}) - (\underline{m} \cdot \underset{\approx}{\mathbf{E}} : \underset{\sim}{\mathbf{P}}). \tag{4.4}$$

This gives the localization condition at the boundary presented by [Benallal *et al.*, 1990 and 1991]:

$$(\underline{m} \cdot \underset{\approx}{\mathbf{E}} \cdot \underline{n})\,(\underline{n} \cdot \underset{\approx}{\mathbf{E}} \cdot \underline{n})^{-1}\,(\underline{n} \cdot \underset{\approx}{\mathbf{E}} \cdot \underset{\sim}{\mathbf{P}}) = \underline{m} \cdot \underset{\approx}{\mathbf{E}} : \underset{\sim}{\mathbf{P}}. \tag{4.5}$$

There results imply that bands in the bulk and bands at the boundary are usually misaligned. Bands of localized deformation may display a kink when approaching a free surface.

For a single crystal undergoing single slip at small strain:

$$\underset{\sim}{\mathbf{P}} = \{\underline{s} \otimes \underline{z}\}. \tag{4.6}$$

By introducing the bifurcation solution $\underline{n} = \underline{z}$, the first part of Eq. (4.5) becomes:

$$(\underline{m} \cdot \underset{\approx}{\mathbf{E}} \cdot \underline{n})\,(\underline{n} \cdot \underset{\approx}{\mathbf{E}} \cdot \underline{n})^{-1}\,(\underline{n} \cdot \underset{\approx}{\mathbf{E}} \cdot \underset{\sim}{\mathbf{P}}) = (\underline{m} \cdot \underset{\approx}{\mathbf{E}} : \underline{n})\,\underline{s} = \underline{m} \cdot \underset{\approx}{\mathbf{E}} : \underset{\sim}{\mathbf{P}} \tag{4.7}$$

so that condition (4.5) is automatically satisfied. A similar proof is available for $\underline{n} = \underline{s}$. This establishes that slip bands and kink bands do not bend when approaching the surface or, conversely, slip bands nucleated at the boundary do no deviate when propagating through the bulk of the single crystal. This is generally not true for the more complicated bifurcation modes associated with continuing multislip within the band and calculated in 2.3 (except for the case of four slip systems).

4.2. Introduction of material imperfections

To trigger the formation of localization bands in finite element calculations, initial geometrical imperfections have been made use of in literature, as in Section 3. In contrast, in the following calculations, we introduce material imperfections in the form of non uniformities of the material parameters involved in the constitutive equations. More specifically, we introduce slightly different values of the elasticity limit locally. For the calculations presented in Figure 6, one element in the bulk of the single crystal plate oriented for single slip ($\underline{x}_3 = [2\ 3\ 8]$, $\underline{x}_1 = [\overline{1}9\ 10\ 1]$) deforms plastically slightly earlier than the surrounding crystal. Figure 6 shows that two orthogonal slip bands form, starting from the material imperfection. Structural effects then result in the predominance of only one of them. The final slip band undergoes no deviation when reaching the free boundary.

5. Effect of interfaces on localization in single crystals

5.1. Bifurcation conditions at an interface

The question now is: what happens at an interface separating two single crystals with differing behaviours due to a slight misorientation (*subgrain boundary*), significant

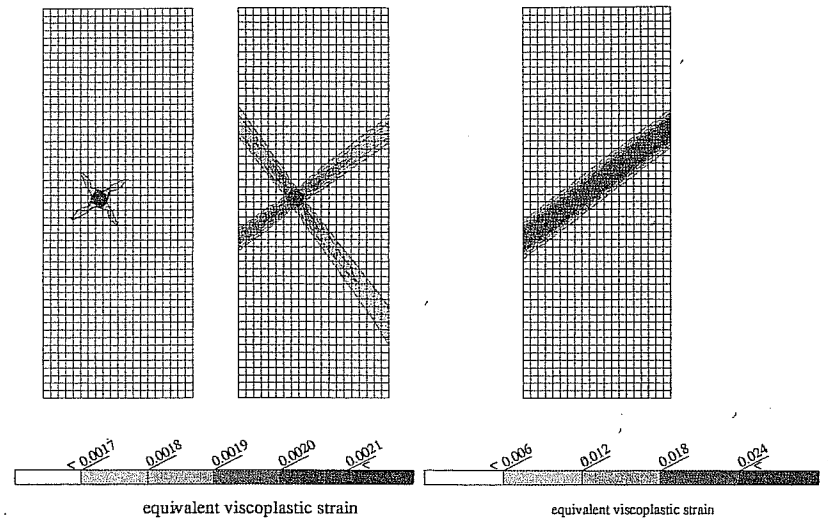

Fig. 6. – Tension of a single crystal plate with a material flaw. (*a*) and (*b*) two bands form starting from the element with a lower elasticity limit, (*c*) only one of them remains at the end.

misorientation (*grains in a polycristal*) or simply different material parameters (see *Fig.* 7)? Bifurcation modes compatible on each side of the interface are of the form:

$$\dot{\underset{\sim}{\varepsilon}}_2 - \dot{\underset{\sim}{\varepsilon}}_1 = \{\underline{g} \otimes \underline{n}\} \tag{5.1}$$

$$\dot{\underset{\sim}{\varepsilon}}'_2 - \dot{\underset{\sim}{\varepsilon}}'_1 = \{\underline{g}' \otimes \underline{n}'\}. \tag{5.2}$$

Continuing equilibrium implies:

$$(\dot{\underset{\sim}{\sigma}}_2 - \dot{\underset{\sim}{\sigma}}_1)\,\underline{n} = 0 \tag{5.3}$$

$$(\dot{\underset{\sim}{\sigma}}'_2 - \dot{\underset{\sim}{\sigma}}'_1)\,\underline{n}' = 0. \tag{5.4}$$

Assuming plastic loading inside and outside the localization band on each side of the interface,

$$\dot{\underset{\sim}{\sigma}}_i = \underset{\approx}{\mathbf{L}}\,\dot{\underset{\sim}{\varepsilon}}_i \qquad \text{for} \quad i \in \{1, 2\} \tag{5.5}$$

$$\dot{\underset{\sim}{\sigma}}'_i = \underset{\approx}{\mathbf{L}}'\,\dot{\underset{\sim}{\varepsilon}}'_i \qquad \text{for} \quad i \in \{1, 2\}. \tag{5.6}$$

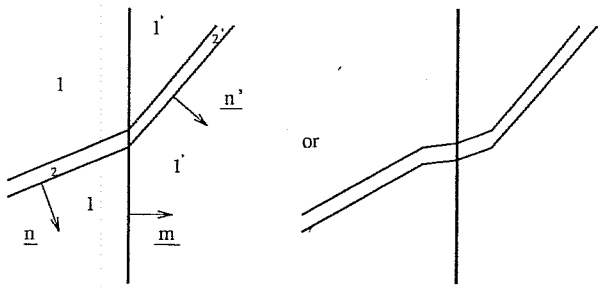

Fig. 7. – Abrupt or diffuse refraction of a localization band at an interface.

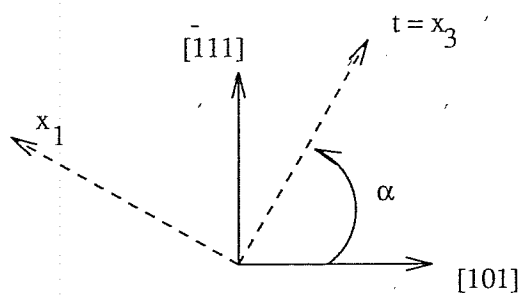

Fig. 8. – Plane single slip configuration.

Equilibrium conditions at the interface imply:

$$\underset{\sim}{\dot{\sigma}}_i \, \underline{m} = \underset{\sim}{\dot{\sigma}}'_i \, \underline{m} \qquad \text{for} \quad i \in \{1, 2\}. \tag{5.7}$$

Eqs. (5.1) to (5.6) lead to the classical bifurcation conditions in the bulk of the material:

$$(\underline{n} \cdot \underset{\approx}{\mathbf{L}} \cdot \underline{n}) \, \underline{g} = 0 \tag{5.8}$$

$$(\underline{n}' \cdot \underset{\approx}{\mathbf{L}}' \cdot \underline{n}') \, \underline{g}' = 0 \tag{5.9}$$

which becomes possible for critical values of the hardening modulus given by (2.14). Interface condition (5.7) implies

$$(\underset{\sim}{\dot{\sigma}}_1 - \underset{\sim}{\dot{\sigma}}_2) \, \underline{m} = (\underset{\sim}{\dot{\sigma}}'_1 - \underset{\sim}{\dot{\sigma}}'_2) \, \underline{m} \tag{5.10}$$

and consequently

$$(\underline{m} \cdot \underset{\approx}{\mathbf{L}} \cdot \underline{n}) \, \underline{g} = (\underline{m} \cdot \underset{\approx}{\mathbf{L}}' \cdot \underline{n}') \, \underline{g}'. \tag{5.11}$$

Since we are interested in the case of single slip, we set $\underset{\sim}{\mathbf{P}} = \{\underline{s} \otimes \underline{z}\}$ and $\underline{n} = \underline{z}$ (resp. $\underline{s}$) and $\underline{g} = \underline{s}$ (resp. $\underline{z}$), and in that condition we have seen in 4.1 that necessarily $(\underline{m} \cdot \underset{\approx}{\mathbf{L}} \cdot \underline{n}) \, \underline{g} = 0$. The same is true on the other side.

This proves that the interface condition for equilibrium (5.11) is automatically fulfilled in the case of single slip bifurcation. Thus, if single slip localization is possible on each side of the interface, equilibrium allows that slip bands do not bend when approaching the interface. The abrupt change of orientation of the bands required by the possible misorientation of the two crystals takes place at the interface without violating local equilibrium.

However, compatibility conditions at the interface are usually not met even before localization. This induces non homogeneous deformation at grain boundaries for instance. Finite element calculations are therefore necessary to see whether these incompatibilities may or not impede the crossing of the interface.

5.2. Bicrystals

Strain incompatibilities caused at small strain by the presence of a grain boundary have been observed experimentally and simulated numerically by Méric *et al.* [1994] for copper bicrystals under cyclic loading. The bicrystals were highly misoriented so that a complex deformation field developped. Deformation modes were rather diffuse and no intense slip band could form.

In contrast, we study here the influence of plastic incompatibilities in bicrystals on the development of slip bands and for that purpose a strain softening behaviour is once more introduced. Such a situation arises in the vicinity of a grain boundary where incipient plasticity can be accompanied with softening mechanisms.

The single crystal plate is now divided into two misoriented single crystals with the same softening behaviour, separated by a perfect interface. The single crystals are oriented for plane single slip so that 2D FE calculations can be performed to reduce computation time. Such a slip configuration is obtained as in Figure 8 where $\underline{x}_1$, $\underline{x}_3$ defining the plate, slip direction [101] and the normal to the slip plane $(\bar{1}11)$ are in the same plane. $\underline{x}_3 = \underline{t}$ is the tensile direction. We take $\underline{x}_3 = \underline{t} = [2\ 3\ 8]$, $\underline{x}_1 = [\bar{1}9\ 10\ 1]$ for the left side, corresponding to $\alpha_{left} = 36.3°$ and we consider first a slight misorientation with $\alpha_{right} = 40°$, that is two subgrains rather than a bicrystal. The right upper corner has a slightly lower elasticity (material imperfection) to trigger the initiation of a slip band in one crystal. The misorientation results in the non homogeneous deformation shown in Figure 9 *a*, that slightly masks the effect of the material imperfection. Nevertheless a slip band initiates at the location of the imperfection and refracted at the interface. Later reflected bands form at the interface (*Fig. 9 b*).

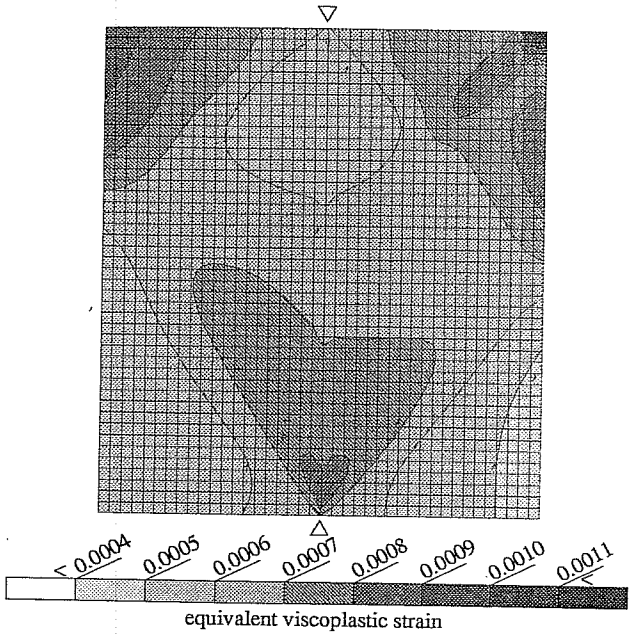

Fig. 9 (*a*). – Tension of a bicrystal. The triangles indicate the interface. The material flaw is located at the upper right corner. Initial contour of viscoplastic strain and initiation of a band.

For a large misorientation $\Delta\alpha = 20°$, the situation is comparable to that of two neighbouring grains. Incompatibility of plastic deformation results immediatly in non homogeneous deformation but does not prevent a slip band from initiating and propagating across the interface with the expected deviation (*Fig.* 10).

5.3. Propagation of a slip band through a hardening zone

We show in this section that a slip band initiated in a softening zone of the single crystal can propagate through surrouding hardening zones. For that purpose we consider once again a rectangular single crystal plate divided into two parts with the same orientation, one displaying a softening behaviour, the other one a hardening behaviour. The upper right corner of the softening part has a slightly weaker elasticity limit so that the initiation of a slip band is expected at this point. The tensile curves corresponding to these different zones are given in Figure 11 *a*. Only single slip is taken into account ($\underline{x}_2 = [2\ 3\ 8]$, $\underline{x}_1 = [\bar{1}9\ 10\ 1]$). Figure 11 *b* shows that a zone of non homogeneous deformation appears starting from the location of the imperfection but the initiating band is repelled at the interface. After that a slip band forms in the softening zone, penetrates slightly the hardening zone (*Fig.* 11 *c*) and finally crosses it (*Fig.* 11 *d*). It is important to notice that conditions for localization considered as a bifurcation mode are not met

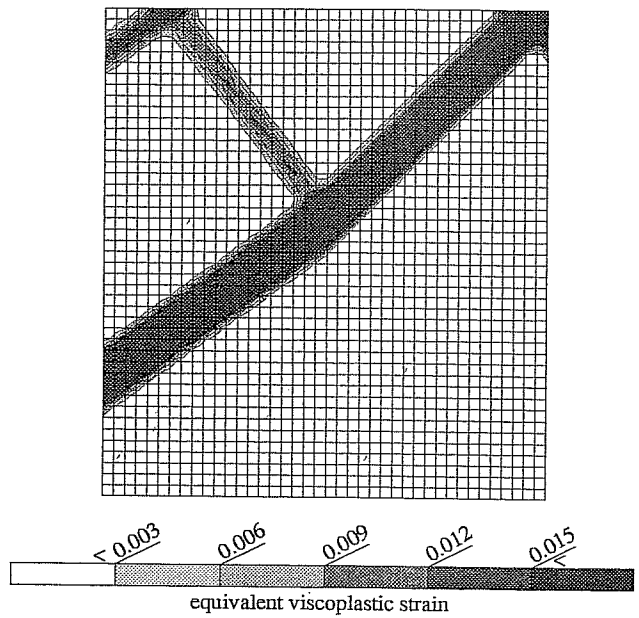

Fig. 9 (*b*). – Tension of a bicrystal: formation of refracted and reflected bands.

in the hardening zone. The propagation of the band through the hardening zone results from structural effects: the material hardens inside the band on the strong side whereas elastic unloading occurs outside (*Figs.* 11 *e* and *f*).

6. Conclusions

The bifurcation analysis performed for single crystals undergoing symmetric multiple slip at small strain shows that the bifurcation planes are crystallographic only in the case of single slip and that softening is required for bifurcation to occur. Some of these localized deformation modes have been obtained using finite element calculations for a one-element thick single crystal plate in tension. The actual three-dimensional slip configurations of f.c.c. single crystals have been taken into account and the occurrence of bifurcation modes induces complex three-dimensional displacement fields. The use of viscoplasticity reduces significantly the mesh dependence of the results. The calculations show also that no special mesh is necessary to capture these complex localization modes.

To trigger localization in the bulk of the specimen, material imperfections have been introduced and account for slightly non-homogeneous material properties. This seems to be of particular physical relevance even though the length scale of these fluctuations remains difficult to assess. The introduction of a softening behaviour is also physically

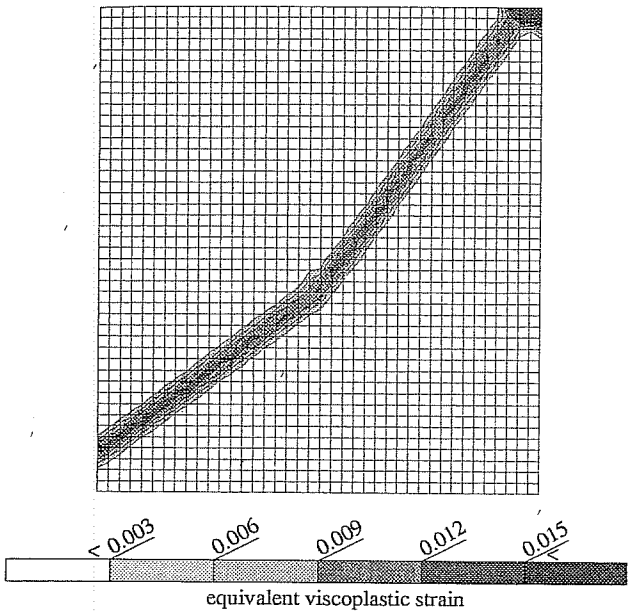

Fig. 10. – Tension of a bicrystal with a significant misorientation of the two crystals: incident and refracted bands.

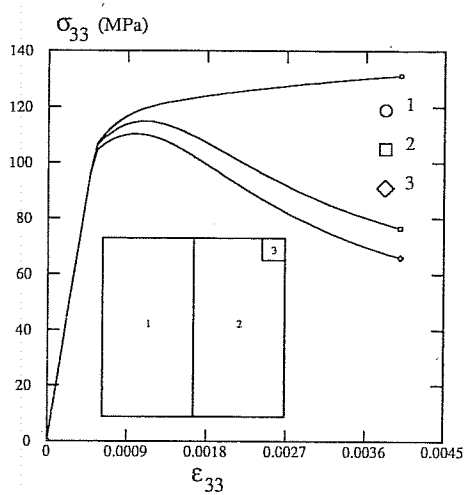

Fig. 11 (*a*). – Tension of a bicrystal composed of grains with the same orientation but different hardening behaviours: behaviour of each part of the mesh.

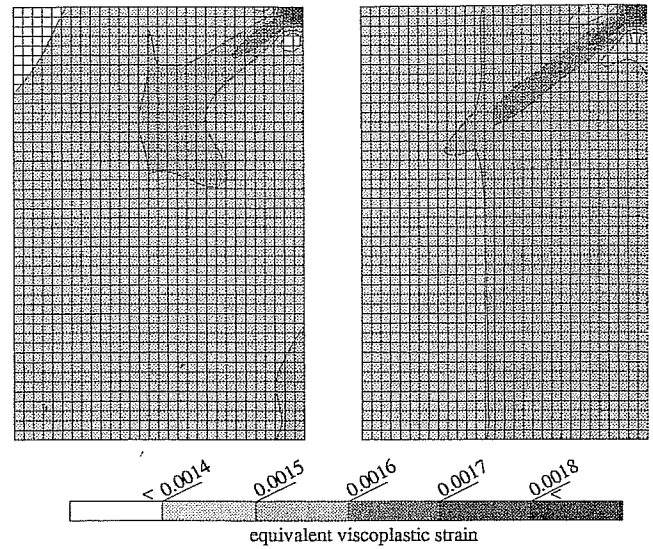

Fig. 11 (*b*) and (*c*). – Initiation of a slip band in the softening zone of the crystal.

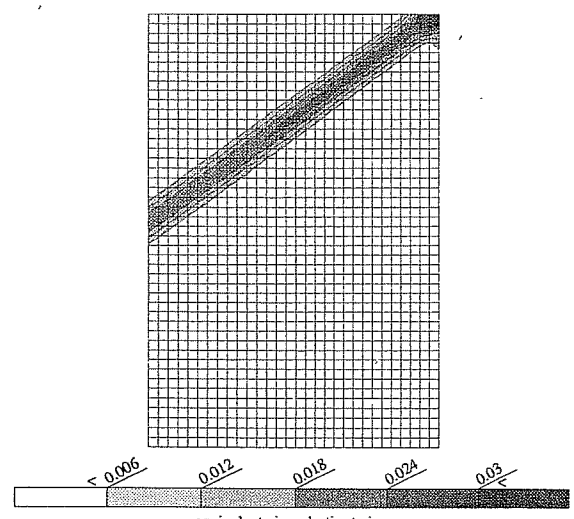

Fig. 11 (*d*). – Crossing of the hardening zone of the crystal by the slip band.

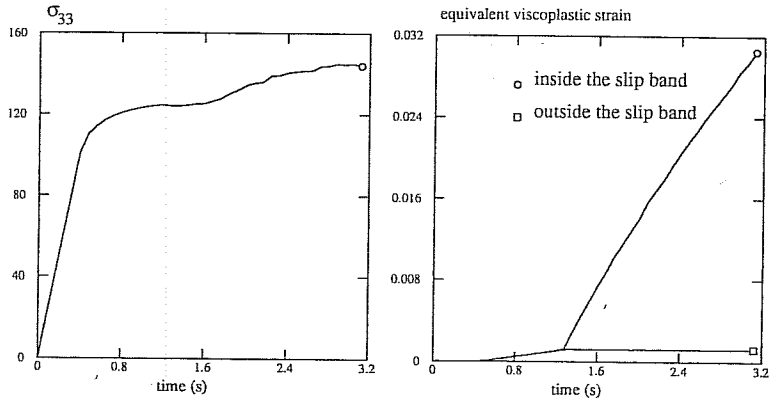

Fig. 11 (*e*) and (*f*). – Evolution of stress and viscoplastic strain in the hardening zone of the crystal.

motivated and is recommended in [Zaoui *et al.*, 1988]. Several physical mechanisms like the shearing of precipitates or the destruction of short range order can induce local softening. Furthermore the non-linear analysis of the evolution of dislocation densities performed by Estrin & Kubin [1986] show that plastic flow is initially an unstable process.

Bifurcation conditions at a boundary and an interface have been applied to the case of single slip. We have proved, on the one hand, that no slip band deviation occurs at a boundary and, on the other hand, that equilibrium conditions allow the crossing of interfaces by slip bands. The crossing of a grain boundary separating two misoriented single crystals has been simulated using the finite element method. Finally the finite element calculations presented in section 5.2 give more insight into the understanding of initiation and propagation of slip bands in single crystals. They show that a slip band initiated in a softening zone of the crystal can cross neighbouring hardening zones and propagate through the entire cross-section of the specimen. This may be accompanied by a serration on the load-displacement curve.

Acknowledgements

This work is part of Brite-Euram project BRE2–CT92–0176. The authors want to thank P. Pilvin for fruitful discussions during this work.

REFERENCES

ASARO R. J., RICE J. R., 1977, Strain localization in ductile single crystals, *J. Mech. Phys. Sol.*, **25**, 309-338.

ASARO R. J., 1979, Geometrical effect in the inhomogeneous deformation of ductile single crystals, *Acta Metall.*, **27**, 445-453.

BENALLAL A., BILLARDON R., GEYMONAT G., 1990, Phénomènes de localisation à la frontière d'un solide, *C. R. Acad. Sci. Paris*, t. 310, Série II, 679-684.

BENALLAL A., BILLARDON R., GEYMONAT G., 1991, Localization at the boundaries and interfaces of solids, *Proc. 3rd Int. Conf. on Constitutive Laws for Engineering Materials*, University of Arizona, Tucson.

BIGONI D., HUECKEL T., 1991, Uniqueness and localization: I associative and nonassociative elastoplasticity, *Int. J. Solids Structures*, **28**, n° 2, 197-213.

BORRÉ G., MAIER G., 1989, On linear versus nonlinear flow rules in strain localization analysis, *Meccanica*, **24**, 36-41.

DE BORST R., 1991, Simulation of strain localization: a reappraisal of the Cosserat continuum, *Eng. Comp.*, **8**, 317-332.

DE BORST R., SLUYS L. J., MÜHLHAUS H. B., PAMIN J., 1993, Fundamental issues in FE analyses of localization of deformation, *Eng. Comp.*, **10**, 99-121.

ESTRIN Y., KUBIN L. P., 1986, Local strain hardening and nonuniformity of plastic deformation, *Acta Metall.*, **34**, n° 12, 2455-2464.

FOREST S., CAILLETAUD G., 1993, Numerical study of localized deformation in elastoviscoplastic materials with application to single crystals, *Twelve monthly progress report*, Brite-Euram project BRE2–CT92–0176, Brussels.

HADAMARD J., 1903, *Leçons sur la propagation des ondes et les équations de l'hydrodynamique*, Hermann, Paris.

HARIRÈCHE O., LORET B., 1991, 3D Dynamic strain-localization: Shear band pattern transition in solids, *Eur. J. Mech., A/Solids*, **12**, n° 6, 733-751.

HILL R., HUTCHINSON J. W., 1975, Bifurcation phenomena in the plane tension test, *J. Mech. Phys. Sol.*, **23**, 239-264.

LEMAITRE J., CHABOCHE J. L., 1985, *Mécanique des matériaux solides*, Dunod, Paris.

MÉRIC L., CAILLETAUD G., 1991, Single crystal modeling for structural calculations; Part 2: finite element implementation, *Journal of Engineering Materials and Technology*, **113**, 171-182.

MÉRIC L., CAILLETAUD G., GASPÉRINI M., 1994, F.E. Calculations of Copper bicrystal specimens submitted to tension-compression tests, *Acta Metall. Mater.*, **42**, n° 3, 921-935.

OTTOSEN N. S., RUNESSON K., 1991, Properties of discontinuous bifurcation solutions in elasto-plasticity, *Int. J. Solids Structures*, **27**, n° 4, 401-421.

PEIRCE D., ASARO R. J., NEEDLEMAN A., 1982, An analysis of non uniform and localized deformation in ductile single crystals, *Acta Metall.*, **30**, 1087-1119.

PEIRCE D., ASARO R. J., NEEDLEMAN A., 1983, Material rate dependence and localized deformation in crystalline solids, *Acta Metall.*, **31**, n° 12, 1951-1976.

PEIRCE D., 1983, Shear band bifurcation in ductile single crystals, *J. Mech. Phys. Solids*, **31**, n° 2, 133-153.

RICE J. R., 1976, The localization of deformation, in *Theoretical and Applied Mechanics*, KOITER W. T. ed., North Holland, Amsterdam, 207-220.

RICE J. R., RUDNICKI J. W., 1980, A note on some features of the theory of localization of deformation, *Int. J. Solids Structures*, **16**, 597-605.

ZAOUI A., KORBEL A., DUBOIS P., REY C., 1988, Bifurcation analysis of shear banding in metals, *Solid State phenomena*, **3 & 4**, 433-446.

(Manuscript received July 20, 1994;
accepted December 12, 1994.)